

Oct 19th, 12:00 AM

Racking Performance of Long Steel-frame Shear Walls

Alexander J. Salenikovich

Daniel J. Dolan

Samuel W. Easterling

Follow this and additional works at: <https://scholarsmine.mst.edu/isccss>



Part of the [Structural Engineering Commons](#)

Recommended Citation

Salenikovich, Alexander J.; Dolan, Daniel J.; and Easterling, Samuel W., "Racking Performance of Long Steel-frame Shear Walls" (2000). *International Specialty Conference on Cold-Formed Steel Structures*. 4. <https://scholarsmine.mst.edu/isccss/15iccfss/15iccfss-session8/4>

This Article - Conference proceedings is brought to you for free and open access by Scholars' Mine. It has been accepted for inclusion in International Specialty Conference on Cold-Formed Steel Structures by an authorized administrator of Scholars' Mine. This work is protected by U. S. Copyright Law. Unauthorized use including reproduction for redistribution requires the permission of the copyright holder. For more information, please contact scholarsmine@mst.edu.

RACKING PERFORMANCE OF LONG STEEL-FRAME SHEAR WALLS

Alexander J. Salenikovich¹, J. Daniel Dolan², and W. Samuel Easterling²

ABSTRACT

The response of cold-formed steel-frame shear walls to lateral forces is the focus of the paper. Results are presented for monotonic and cyclic tests of sixteen full-size shear walls with and without openings. Walls of five configurations with sheathing area ratio ranging from 1.0 to 0.3 were tested. The specimens were 12-m (40-ft.) long and 2.4-m (8-ft.) high with 11-mm (7/16-in.) oriented strandboard (OSB) sheathing. One specimen had additional 13-mm (0.5-in.) gypsum wallboard sheathing. All specimens were tested in horizontal position with no dead load applied in the plane of the wall. Resistance of walls was compared with predictions of the perforated shear wall design method. During monotonic and cyclic tests, steel-frame walls failed in a stepwise manner due to bending of framing elements and head pull-through of sheathing screws. No fatigue of mechanical connections was observed. Cyclic loading did not affect elastic performance of the walls but significantly reduced their deformation capacity. Fully-sheathed walls were significantly stiffer and stronger but significantly less ductile than walls with openings. Gypsum sheathing was additive to the stiffness and strength of fully-sheathed walls during monotonic tests. Predictions of the perforated shear wall method appeared to be conservative at all levels of loading when overturning anchors are present at the ends of the wall specimen.

INTRODUCTION

Light-frame shear walls are a primary element in the lateral force-resisting system in residential construction. Traditional design of exterior shear walls containing openings for windows and doors, accounts for strength of fully-sheathed shear wall segments only. Each full-height shear wall segment is required to have overturning restraint supplied by structure weight and/or mechanical anchors. The shear capacity of a wall must equal the sum of the individual full-height segment shear capacities, and sheathing above and below openings is not considered to contribute to the overall performance of the wall. Shear wall design values for segmented walls of cold-formed steel construction have been included in the three model building codes for the United States. The design values are based on monotonic and cyclic tests conducted by Serrette, et al. (1996, 1997) on 2.4 × 2.4 m (8 × 8 ft.) and 1.2 × 2.4 m (4 × 8 ft.) specimens sheathed with plywood, OSB, and gypsum.

The perforated shear wall method is an alternate empirical-based approach to the design of wood-framed shear walls with openings. This method appears in the *Standard Building Code 1996 Revised Edition* (SBC 1996), the *International Building Code* final draft (IBC 1998), and the *Wood Frame Construction Manual* (WFCM) (AF&PA 1995). The perforated shear wall method consists of a combination of prescriptive provisions and empirical adjustments to design values in shear wall selection tables for the design of shear wall segments containing openings. Shear walls designed using this method, must be anchored only at the wall ends, not at each wall segment.

If similar sheathing materials and fasteners are used for wood- and steel- frame shear walls, it is reasonable to assume similar performance for both types of frames. This study was conducted to confirm that the perforated shear wall method for design of shear walls is valid for cold-formed steel shear walls. Results of monotonic and cyclic tests of full-size cold-formed steel-frame shear walls meeting the requirements of the perforated shear wall method are reported. Monotonic tests serve as a basis for establishing design values in wind design. Cyclic tests are performed to establish conservative estimates of performance during a seismic event.

The objectives of the study were to determine the effects of (a) size of openings, (b) cyclic loading, (c) gypsum drywall sheathing on steel-framed shear wall performance, and to compare the strength of walls with predictions of the perforated shear wall method.

¹ Graduate Research Assistant, Virginia Polytechnic Institute and State University, Blacksburg, VA

² Associate Professor, Virginia Polytechnic Institute and State University, Blacksburg, VA

BACKGROUND

The perforated shear wall design method for wood-frame shear walls appearing in the SBC, IBC, and WFCM is based on an empirical equation, which relates the strength of a shear wall segment with openings to one without openings. Adjustment factors are used to reduce the strength or increase the required length of a traditional fully-sheathed shear wall segment to account for the presence of openings.

Prescriptive provisions and empirical adjustments are based on results of various studies conducted on shear walls with openings. Many of the prescriptive provisions are necessary to meet conditions for which walls in previous studies were tested. Empirically derived adjustment factors, or shear capacity ratios, for the perforated shear wall method have roots in works of Japanese researchers. To determine the shear capacity ratio, Sugiyama and Matsumoto (1993) defined the sheathing area ratio:

$$r = \frac{1}{1 + \frac{A_0}{H \sum L_i}} \quad (1)$$

where: $A_0 = \sum A_i$, total area of openings, H = height of wall, and $\sum L_i$ = sum of the length of full-height sheathing as shown in Figure 1.

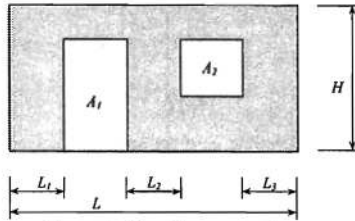


Figure 1 - Sheathing area ratio.

Initially, Yasumura and Sugiyama (1984) proposed the following equation for the shear load ratio (F), or the ratio of the resistance of a shear wall with openings to the resistance of a fully-sheathed shear wall without openings:

$$F = \frac{r}{3 - 2r} \quad (2)$$

The relationship was derived based on results of monotonic racking tests on 1/3-scale wood-framed walls and was considered applicable for the apparent shear deformation angle of 1/100 radian and for ultimate load. Later, Sugiyama and Matsumoto (1994) published two more equations based on tests of longer wall models and suggested for use in North-American wood-frame construction:

$$F = \frac{3r}{8 - 5r} \quad (3)$$

for the shear deformation angle $\gamma = 1/300$ radian, and

$$F = \frac{r}{2 - r} \quad (4)$$

for $\gamma = 1/100$ and 1/60 radian.

It follows from above that the load ratio F depends on the wall deflection. Tabulated shear load ratios or opening adjustment factors appearing in the SBC and WFCM are based on Equation (2) assuming that the height of all openings in a wall are equal to the largest opening height. The result is that SBC and WFCM tabulated shear capacity ratios or opening adjustment factors for walls containing openings of varying height are smaller than would be calculated using Equation (2) and, therefore, the method included in the code is more conservative. The WFCM uses a full-height sheathing length adjustment factor in the application of Equation (2) to design. The adjustment factor depends on the maximum opening height in the wall, and is multiplied by the length of wall required if there are no openings present.


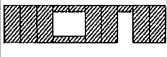



Johnson (1997) tested 12.2-m (40-ft.) long timber frame walls of five configurations with sheathing area ratio varying from 0.3 to 1.0. A wall of each configuration was tested once monotonically and once cyclically. The specimens were constructed in accordance with the requirements of the perforated shear wall design method (i.e. tie-down anchors applied at the wall ends). Structural 12-mm (15/32-in.) plywood sheathing was attached on one side and 13-mm (1/2-in.) gypsum wallboard on the other. Heine (1997) tested three of the same configurations monotonically and cyclically with 11-mm (7/16-in.) oriented strandboard (OSB) instead of plywood. Both studies proved Equation (2) conservative in predicting both monotonic and cyclic capacities of long shear walls.

TEST PROGRAM

Specimens

Monotonic and cyclic tests were conducted on steel-framed walls of each configuration shown in Table 1. Size and placement of openings were selected to cover the range of sheathing area ratios encountered in light-frame construction. Walls A had no openings and were included in the investigation for referencing the performance of walls with openings.

Table 1 - Wall configurations and sheathing area ratio, (r).

A ($r = 1.0$)	B ($r = 0.76$)	C ($r = 0.56$)	D ($r = 0.48$)	E ($r = 0.30$)
				

The specimens were built in accordance with the *Builder's Steel-Stud Guide* (AISI 1996) and framed and sheathed to provide the weakest condition that still conformed to the design specification. All specimens were 12.2-m (40-ft.) long and 2.4-m (8-ft.) tall with the same type of framing, sheathing, fasteners, and fastener schedules. Wall framing consisted of single top and bottom tracks, single intermediate and double end-studs, and double studs around doors and windows. All frame members consisted of cold-formed steel profiles. Exterior sheathing was 11-mm (7/16-in.) OSB. All full-height panels were 1.2×2.4-m (4×8 ft.) and oriented vertically. Interior 13-mm (1/2-in.) gypsum wallboard sheathing in 4×8-ft. sheets oriented vertically was applied on an additional monotonic test of wall A. All joints in the interior sheathing were taped and covered with drywall compound. Self-drilling sheathing screws were spaced 152 mm (6 in.) on perimeter and 305 mm (12 in.) in field to attach OSB sheathing, and 178 mm (7 in.) on perimeter and 254 mm (10 in.) in field for gypsum wallboard. A minimum edge distance of 9.5 mm (3/8 in.) was maintained for all fasteners. Further manufacturing details can be found in Salenikovich, et al. (1999).

Test Setup

Tests were performed with the shear walls in a horizontal position, with the OSB sheathing on top. In this setup, no dead load was applied in the plane of the wall, which conservatively represented walls parallel to floor joists. Racking load was applied to the top left corner of the wall (for the configurations shown in Table 1) by a programmable servo-hydraulic actuator with the range of displacement of ± 152 mm (6 in.) and capacity of 245 kN (55 Kips). Specimens were attached to 76×127-mm (3×5-in.) steel tubes at the top and the bottom with 15.9-mm (5/8-in.) diameter bolts at 610 mm (24 in.) on center. Two tie-down anchors were used, one at the bottom of each double stud at the wall ends. Load was distributed along the length of the wall by means of the steel tube attached to the top plate of the wall. Eight casters were attached to the distribution beam parallel to the loading direction to allow free horizontal motion. The hydraulic actuator contained the load cell and internal LVDT that supplied information on applied force and displacement. Data were recorded at a frequency 10 Hz in monotonic tests and 20 Hz in cyclic tests.

Load Regimes

Two load regimes were used in testing the walls: monotonic and cyclic. Monotonic load was applied at the rate of 15 mm/min (0.6 in./min). Without unloading, the deflection progressively increased from zero to 152 mm (6 in.). For cyclic tests, a sequential phased displacement (SPD) procedure, adopted by the Structural Engineers Association of Southern California (SEAOSC 1997) was used. To define the displacement pattern, the yield displacement (first major event) was assumed at 2.5 mm (0.1 in.). The excitation was a triangular reversing ramp function at a frequency of 0.4 Hz as illustrated in Figure 2.

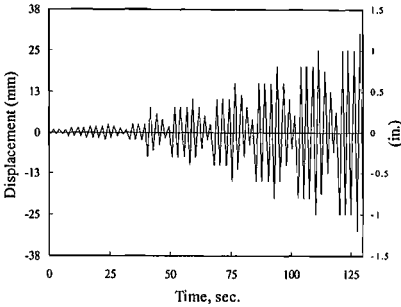


Figure 2. - SPD loading procedure.

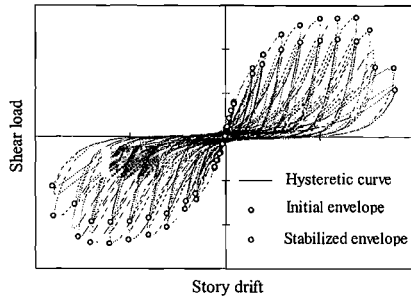


Figure 3. - Typical cyclic response curve.

TEST RESULTS AND DISCUSSION

Definition of performance parameters

Sixteen specimens were constructed and tested for this study. One monotonic and two cyclic tests were performed on each wall configuration. In addition, one wall with interior and exterior sheathing was tested monotonically to determine the effect of gypsum wallboard. For analysis of monotonic tests, observed response curves were used. For analysis of cyclic tests, so-called *envelope response curves* were produced. The hysteresis curve in Figure 3 represents a typical load-deflection response observed during the cyclic tests. Two envelope curves, as shown in Figure 3, are obtained from the hysteresis curve: one for the first and the other for the last cycle in each phase of the loading. These curves are referred to as *initial* and *stabilized* response curves and are analyzed like the monotonic response curves. Since the envelope curves include reversed sides, the absolute values of parameters of the negative and the positive curves are averaged during the analysis.

Wall load and deflection at capacity (V_{peak} and Δ_{peak}), deflection at $0.4V_{peak}$, and failure point ($V_{failure}$, $\Delta_{failure}$) are determined for each monotonic, initial, and stabilized response curve using a plot similar to that shown in Figure 4. The failure point is considered at $0.8 V_{peak}$ (i.e., when a 20% decrease in resistance occurs). The area under the curve limited by the failure point approximates the work that can be done by the wall during a monotonic test. Using these data, the *equivalent energy elastic-plastic* (EEEP) curve is derived for each specimen, as is shown in Figure 4. The initial slope of the EEEP curve, drawn through $0.4V_{peak}$ on the observed curve, determines the elastic stiffness (k_e) of the wall. The yield point (V_{yield} , Δ_{yield}) is found by equating the areas under the observed and EEEP curves. The bilinear EEEP curves obtained this way allow comparison of the nonlinear performance of different walls on an equivalent energy basis.

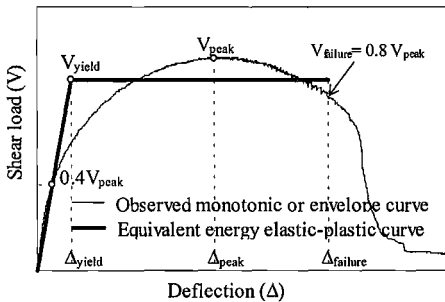


Figure 4 - Performance parameters.

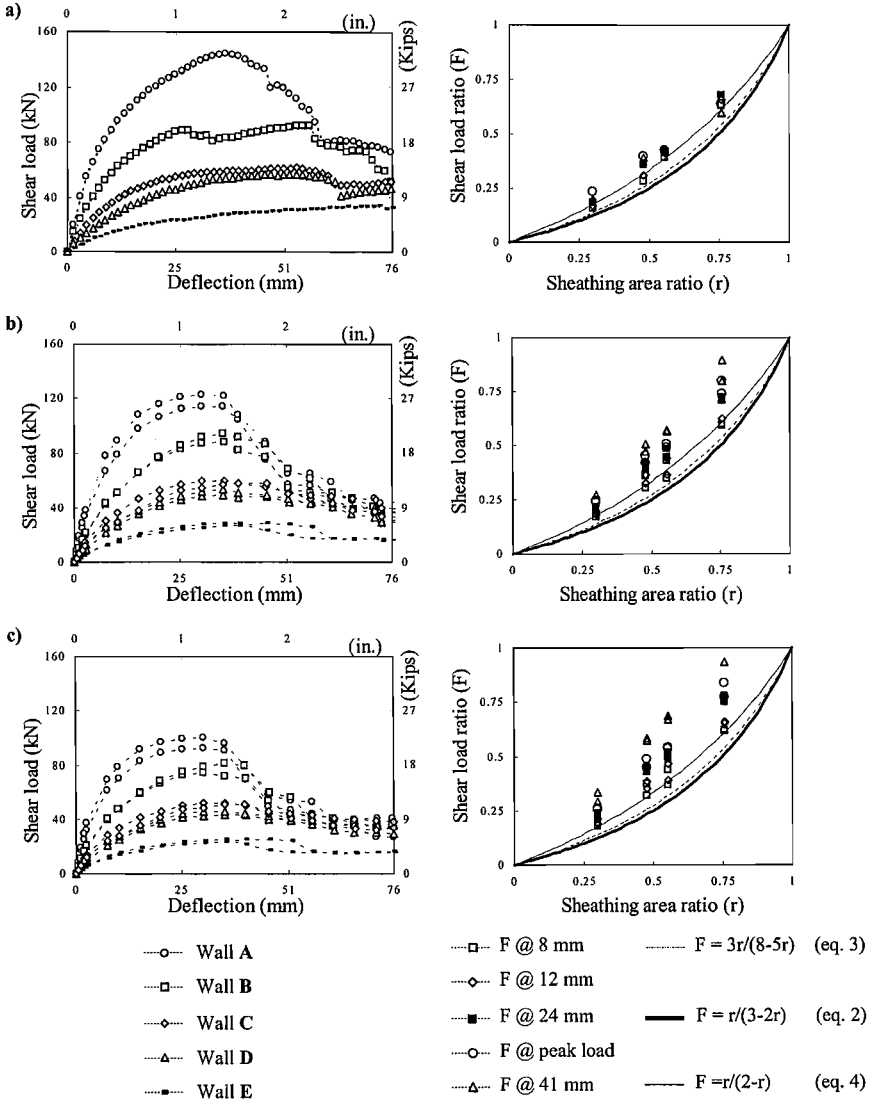


Figure 5 - Response curves and shear load ratios of walls with various openings:

- a) monotonic response
- b) initial cyclic response
- c) stabilized cyclic response

Effects of opening size

To illustrate the response of walls with various opening sizes under monotonic and cyclic loading, Figure 5 shows load-deflection curves (on the left side) and shear load ratios at various levels of deflection (on the right side). The shear load ratio (F) is shown as a function of sheathing area ratio (r). Lines represent predictions of shear load ratios given by Equations (2), (3), and (4). Markers represent the experimental values of F estimated at various deflection points. For example, circles and black squares show the load ratio F at the peak load and at 24-mm (0.96-in.) deflection, respectively, for walls with various areas of openings. All the markers are above the bold line representing the prediction equation (2) used in the design codes to determine shear wall strength. Results suggest that Equation (2), as well as Equation (3), produced overly conservative estimates. At all levels of deflection under monotonic and cyclic loading, the resistance of each specimen significantly exceeded values predicted by these equations. For both load regimes, the closest predictions were obtained at the early stages of deflection using Equation (4). The shear load ratios at 8 mm (0.32 in.) and 12 mm (0.48 in.) deflections were predicted with $\pm 15\%$ accuracy. At higher deflection levels, the estimates of Equation (4) also came out conservative and increased in conservatism with cycling at amplitudes beyond yield point.

The reasons for obtaining the high shear load ratios can be explained using Table 2, which summarizes performance parameters obtained from the analysis of the response curves. Although fully sheathed walls (A) were significantly stiffer than walls with openings, they were also less ductile. Walls A reached capacity and degraded earlier than other walls, especially in cyclic tests. Comparisons of elastic stiffness and yield points indicate that walls with larger openings were less stiff under both monotonic and cyclic load conditions. This is why these walls had higher displacement capability. Similar trends were characteristic of wood-frame walls tested by Johnson (1997) and Heine (1997).

Table 2 - Performance parameters of walls with various openings.

Parameter	Load condition	Units	Wall configuration				
			A	B	C	D	E
V_{peak}	monotonic	Kips	32.5	20.7	13.9	12.8	7.7
	cyclic initial		26.7	20.5	13.3	11.6	6.5
	cyclic stabilized		21.7	17.5	11.7	10.1	5.6
Δ_{peak}	monotonic	in.	1.49	2.19	2.09	1.84	2.85
	cyclic initial		1.31	1.41	1.49	1.51	1.66
	cyclic stabilized		1.16	1.30	1.46	1.46	1.50
V_{yield}	monotonic	Kips	28.1	18.5	12.6	11.6	6.7
	cyclic initial		24.1	18.2	11.8	10.3	5.7
	cyclic stabilized		19.6	15.5	10.3	9.0	4.9
Δ_{yield}	monotonic	in.	0.41	0.46	0.54	0.76	0.82
	cyclic initial		0.38	0.54	0.54	0.56	0.58
	cyclic stabilized		0.30	0.47	0.49	0.51	0.51
Δ_{failure}	monotonic	in.	2.05	2.55	2.44	2.51	4.31
	cyclic initial		1.68	1.90	2.43	2.37	2.07
	cyclic stabilized		1.58	1.75	2.20	2.39	1.93
k_e	monotonic	Kip/in.	68.4	40.5	23.4	15.3	8.3
	cyclic initial		64.1	33.7	21.9	18.5	9.8
	cyclic stabilized		66.7	33.1	21.1	18.0	9.6

Note: 1Kip = 4.448 kN, 1in. = 25.4 mm.

Effects of cyclic loading

Generally, elastic performance of the walls under cyclic loading was comparable to that under monotonic regime despite high variation. Elastic stiffness deviated in both directions less than 20%. Major differences took place in the yield zone. Various performance parameters were influenced to a different

degree depending on the wall configuration. In comparison with other parameters, cyclic loading affected wall deflections at peak load most of all. Stabilized cyclic capacity developed at 53% to 68% of corresponding deflections in monotonic tests. Walls A and E were the most sensitive to cyclic loading. Cyclic response of intermediate wall configurations was least influenced. Initial cyclic capacities of walls A and E were 82% to 84% of the monotonic values, while the corresponding parameters of walls B, C, and D decreased less than 10%. Although, $\Delta_{failure}$ varied in a wide range, it was affected by as much as 50% in cyclic tests when compared to monotonic tests. Stabilized resistance of walls was affected to a greater extent than initial. Relative to initial values, stabilized capacity and yield load were 19% lower for walls A and 13% to 15% lower for all other walls. Consequently, stabilized strength of walls was up to 33% lower than in monotonic tests. Stabilized deformation parameters and elastic stiffness were generally similar to initial response parameters because major events took place in the same phase of excitation, i.e. at the same amplitude. Reduced deflections for cyclic performance were similar in magnitude to those observed by Johnson (1997) for wood-framed walls.

One reason for the early failure of walls in cyclic tests was due to extreme energy demands imposed by the SPD procedure. Table 3 gives comparison of energy dissipated by walls until failure during monotonic and cyclic tests. As a rule, it took more than 100 cycles and more than 8 times the energy of the monotonic test to destroy a wall during cyclic tests. The severity of the SPD protocol manifests itself in steel-frame shear walls by excessive damage to the OSB sheathing around the screw head. The small bugle head of the screws pulled through the sheathing. Some of the damage may have been minimized if screws with a larger and different shaped head were used. A larger head would have increased the resistance to screw head pull through and associated higher shear wall capacity.

Table 3 - Energy dissipated by walls until failure (Kip-ft.).

Load condition	Wall configuration				
	A	B	C	D	E
monotonic	4.3	3.6	2.3	2.1	2.2
cyclic	32.0	30.5	31.0	19.7	10.1
cyclic / monotonic	740%	853%	1365%	956%	463%

Note: 1Kip = 4.448 kN, 1ft. = 0.3048 m.

Effects of gypsum sheathing and steel framing

Performance parameters of walls with interior gypsum wallboard sheathing (**Amongyp**) and without it (**Amon**) under monotonic loading are shown in Table 4. The data show that wall **Amongyp** was 39% stiffer and 24% stronger than wall **Amon**. However, the peak load was reached at a 22% smaller deflection. Note that both walls failed immediately after deflection exceeded 52 mm (2 in.). Based on monotonic tests of wood-frame fully-sheathed walls, other researchers (Patton-Mallory, et al 1984, Rose and Keith 1996) supported the conclusion about the additive strength of gypsum wallboard and structural sheathing. Results reported by Serrette, et al. (1996) and our results indicate that the effect of adding gypsum wallboard is similar for monotonic loading of steel-frame walls.

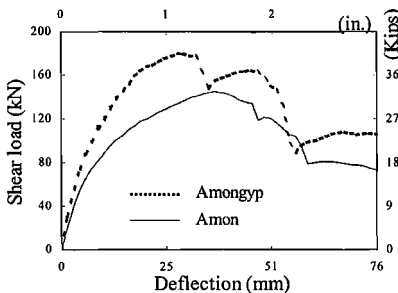


Figure 6 - Load-deflection curves of walls A with and without gypsum sheathing.

Table 4 - Performance parameters of walls A with and without gypsum sheathing.

Parameter	Units	Amon	Amongyp
V_{peak}	Kips	32.5	40.3
Δ_{peak}	in.	1.49	1.16
V_{yield}	Kips	28.1	35.5
Δ_{yield}	in.	0.41	0.37
$\Delta_{failure}$	in.	2.05	2.06
k_e	Kip/in.	68.4	94.9
W^1	Kip-ft.	4.3	5.5

¹: Energy dissipated at failure ($\Delta_{failure}$).
Note: 1Kip = 4.448 kN, 1in. = 25.4 mm.

General observations

Note in Figure 6 that the monotonic curves of steel-frame walls descend in a stepwise manner after capacity is exceeded. These steps might be because the load increased while edges of adjacent panels bore against each other. The load dropped as soon as the row of fasteners along one of the panel edges failed entirely and the sheathing overlapped (as illustrated in Figure 7), causing a sudden loss in resistance.

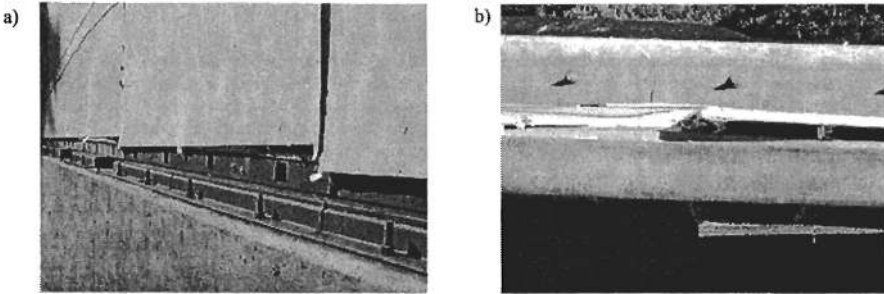


Figure 7 - Failure of wall **Amongyp**: a) view at the bottom plate, b) view from the top plate.

Steel frames racked without separation of studs from the tracks due to pivoting of the stud ends around framing screws. Such assembly was relatively stiff because it engaged all sheathing screws and panel edges into load resistance. Deflection demand on the sheathing connections increased until screws tore through the edge of the sheathing or pulled heads through the sheathing panel. While framing connections of steel-frame walls appeared strong, the framing elements suffered from low bending rigidity. Figure 8 shows that tracks experienced significant bending especially at the wall ends. The more sheathing a wall had, the more bending demand was applied to the studs by adjacent panel connections, which resulted in buckling of the studs. The buckling occurred near openings in the web of the studs.

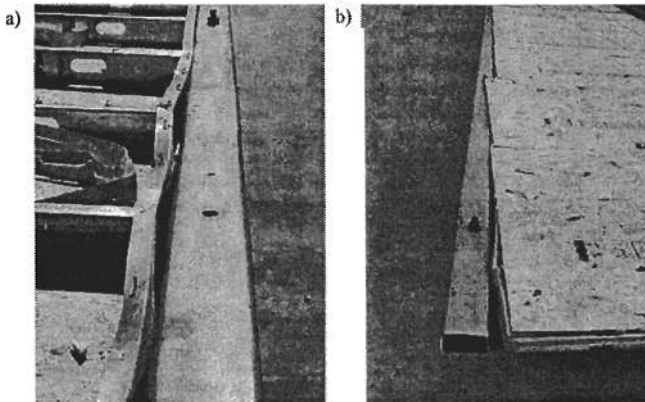


Figure 8 - Bending of top plates: a) wall **Amongyp**, b) wall **Amon**.

The predominant failure mode of steel-frame walls was head pull-through of sheathing screws and bending of frame elements. None of the framing screws failed, which kept the framing connections essentially intact (except for crushing of the stud ends). For this reason, the height of the wall remained relatively constant throughout the test and allowed symmetrical pivoting of sheathing panels with arbitrary 'unzipping' of sheathing connections along either top or bottom plates, as well as along studs. This indicates that the sheathing screws had load distributed to them in a uniform manner.

Flanges of the light-gage profile held sheathing screws in a way that made them work by pivoting in the flanges. Due to pivoting, no sheathing screws failed in fatigue. The resistance of such pinned connections was governed by the ability of side members (sheathing) to hold the screw heads. Figure 9 shows typical failure modes of sheathing connections. Using larger screw heads would probably result in significantly higher stiffness and strength.

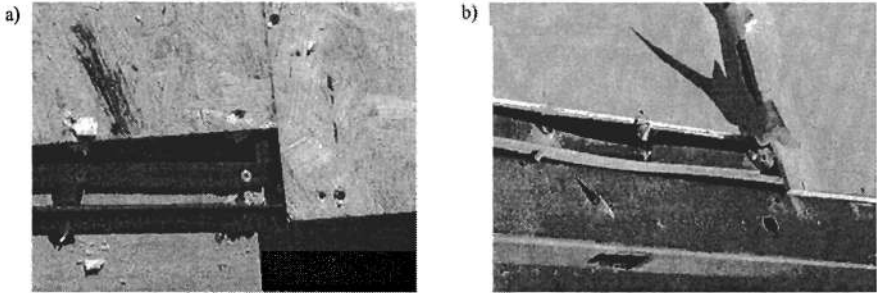


Figure 9 - Typical failure modes of sheathing connections: a) OSB, b) gypsum wallboard.

CONCLUSIONS

Based on results of sixteen monotonic and cyclic tests of 12-m (40-ft.) long steel-frame shear walls with and without openings, the following conclusions were made:

- 1) Comparison of steel-frame wall resistance with predictions of the perforated shear wall method and Sugiyama's equations revealed the conservative nature of the predictions at all levels of monotonic and cyclic loading. With the capacity of the 12-m (40-ft.) fully-sheathed wall taken as a reference, Equation (4) produced the closest estimates in the elastic range. However, the use of Equation (2), as used in the building codes, is more conservative and will provide acceptable prediction of shear wall strength for both monotonic and cyclic loading of cold-formed steel shear walls.
- 2) Long, fully-sheathed walls were significantly stiffer and stronger but less ductile than walls with openings.
- 3) Cyclic loading did not affect elastic performance of the walls but reduced their deformation capacity ($\Delta_{failure}$). Similar reductions in displacement capacity were observed during equivalent tests of wood-framed walls.
- 4) Stabilized cyclic strength of walls was up to 19% lower than initial cyclic and up to 33% lower than monotonic capacities. Strength of fully sheathed walls was affected by cyclic loading more than walls with openings. Similar results were observed by Johnson (1997) for wood-framed walls.
- 5) In monotonic tests, elastic stiffness and strength of fully sheathed walls increased approximately 39% and 24%, respectively, when gypsum sheathing was applied and the fasteners were spaced at 6 inches for the OSB sheathing.
- 6) Monotonic capacity of fully-sheathed steel-frame walls was comparable to that of wood-frame walls.
- 7) In monotonic and cyclic tests, steel-frame walls degraded in abrupt, stepwise manner due to bending of framing elements and pulling heads of sheathing screws through sheathing arbitrarily along the studs or top and bottom tracks. Sometimes, sheathing screws tore through panel edges. No fatigue of mechanical connections was observed.

REFERENCES

American Forest & Paper Association (AF&PA), 1995, *Wood Frame Construction Manual for One- and Two- Family Dwellings - SBC High Wind Edition*, AF&PA, Washington, D.C.

- American Iron and Steel Institute (AISI), 1996, *Builder's Steel Stud Guide*, Publication RG-9607, AISI, Washington, D.C.
- Building Seismic Safety Council (BSSC), 1997, *NEHRP Recommended Provisions for Seismic Regulations for New Buildings and Other Structures*, BSSC, Washington, D.C.
- Heine, C. P., 1997, *Effect of Overturning Restraint on the Performance of Fully Sheathed and Perforated Timber Framed Shear Walls*, Thesis submitted in partial fulfillment of Master's of Science Degree in Civil Engineering, Virginia Polytechnic Institute and State University, Blacksburg, VA
- International Code Council, 1998, *International Building Code 2000, Final Draft*, ICC, Falls Church, VA
- International Conference of Building Officials (ICBO), 1997, *Uniform Building Code*, ICBO, Whittier, CA
- Johnson, A. C., 1997, *Monotonic and Cyclic Performance of Full-Scale Timber Shear Walls with Openings*, Thesis submitted in partial fulfillment of Master's of Science Degree in Civil Engineering, Virginia Polytechnic Institute and State University, Blacksburg, VA
- Patton-Mallory, M., Gutkowski, R. M., and Soltis, L. A., 1984, *Racking Performance of Light-Frame Walls Sheathed on Two Sides*, Research paper FPL 448, USDA Forest Service, Forest Products Laboratory, Madison, WI
- Rose, J. D. and E. L. Keith, 1996, *Wood Structural Panel Shear Walls with Gypsum Wallboard and Window/Door Openings*, APA Research Report 157, APA – The Engineered Wood Association, Tacoma, WA
- Salenikovich, A. J., J. D. Dolan, and W. S. Easterling, 1999, *Monotonic and Cyclic Tests of Long Steel-Frame Shear Walls with Openings*. Virginia Polytechnic Institute and State University Timber Engineering Report TE-1999-001, Blacksburg, VA
- Serrette, R., G. Hall, and J. Ngyen, 1996, *Shear Wall Values for Light Weight Steel Framing, Light Gauge Steel Research Group*, Report No. LGSRG-3-96, Santa Clara University, Santa Clara, CA.
- Serrette, R., J. Encalada, G. Hall, B. Matchen, H. Nguyen, and A. Williams, 1997, *Additional Shear Wall Values for Light Weight Steel Framing, Light Gauge Steel Research Group*, Report No. LGSRG-1-97, Santa Clara University, Santa Clara, CA.
- Standard Building Code*, 1994 with 1996 Revisions, Southern Building Code Congress International, Birmingham, AL.
- Structural Engineers Association of Southern California (SEAOSC), 1997, *Standard Method of Cyclic (Reversed) Load Tests for Shear Resistance of Framed Walls for Buildings*, SEAOSC, Whittier, CA
- Sugiyama, H. and T. Matsumoto, 1993, *A Simplified Method of Calculating the Shear Strength of a Plywood-Sheathed Wall with Openings II. Analysis of the Shear Resistance and Deformation of a Shear Wall with Openings*, *Mokuzai Gakkaishi*, 39(8): 924-929
- Sugiyama, H. and T. Matsumoto, 1994, *Empirical Equations for the Estimation of Racking Strength of a Plywood-Sheathed Shear Wall with Openings*. *Transactions of the Architectural Institute of Japan*
- Yasumura, M. and H. Sugiyama, 1984, *Shear properties of plywood-sheathed wall panels with opening*. *Transactions of the Architectural Institute of Japan*, 338(4), 88-98

APPENDIX – NOTATION

The following symbols were used in this paper:

- | | |
|--|--|
| A_i = area of an opening in shear wall; | V = shear load resisted at the top of the wall (in cyclic tests: average of absolute values on positive and negative strokes); |
| A_0 = total area of openings in shear wall; | W = energy dissipated at failure; |
| F = shear load ratio; | Δ = lateral displacement of the top of shear wall (in cyclic tests: average of absolute values on positive and negative strokes). |
| H = height of shear wall; | |
| k_e = elastic stiffness of shear wall (at $0.4V_{peak}$); | |
| L_i = length of a fully-sheathed segment; | |
| r = sheathing area ratio; | |